

## Shot Noise Measurement in $p-i-n$ Diode and Its Analysis

K. Hara, O. Matsushima, G. Suzuki, D. Navarro, K. Konno, Y. Isobe, and M. Miura-Mattausch

*Graduate School of Advanced Sciences of Matter,  
Hiroshima University, Higashi-Hiroshima 739-8530, Japan*

Phone: +81-82-424-7637, FAX: +81-82-424-7638, E-mail: kiyohito@hiroshima-u.ac.jp

### 1. Introduction

Noise is becoming more serious as device size approaches its limit to improve its high-frequency performance. Among them, the  $1/f$ - and the thermal-noise have been intensively studied experimentally and theoretically. Another type of noise, namely the shot noise, is also expected to become unnegligible. Origin of the shot noise is current fluctuation due to potential barrier. Advanced technologies such as pocket implantation at contact and enhanced dopant fluctuation caused by ion implantation, impose high possibility of inducing barriers. Nevertheless, very few works[1] have been done so far to investigate shot noise. In this paper, we investigate experimentally the noise originating from a lateral  $p-i-n$  diode, where the shot noise is expected to be measurable due to the presence of a potential barrier. We show that shot noise is responsible for noise enhancement in the high-frequency region with low applied biases.

### 2. Noise Measurement and Analysis

We fabricated  $p-i-n$  diode with  $p^+$  and  $n^+$  impurity concentration of  $10^{20}\text{cm}^{-3}$ . The substrate is a  $p$ -type Si with  $10^{15}\text{cm}^{-3}$  impurity concentration. The cross section of the device is shown in Fig. 1. Fig. 2 shows measured  $I$ - $V$  characteristics of the device. The measurement is reproduced by performing simulation analysis of the same device structure in the 2D-device simulator MEDICI [2]. The solid line shows the simulation result considering diffusion and drift contributions. To reproduce the measurement recombination contribution (dashed curve) was required. It is seen that, recombination current dominates at lower bias. Thus fluctuation of the recombination current is observed as the shot noise. The initial hump in the measured  $I$ - $V$  is attributed to some kind of defect introducing leak currents.

The measured current noise power spectrum density  $S_i$  as a function of frequency for forward-biased ( $V_{pn}$ )  $p-i-n$  diode is shown in Fig. 3. At low frequency the well-known  $1/f$  characteristics is observed. At higher frequency,  $S_i$  reduces to constant at higher  $V_{pn}$  values, while it becomes larger at about 10KHz for lower  $V_{pn}$  values.

Following the shot noise expression[3]

$$S_i \simeq 4kTg_0 \left[ \frac{1}{2} + \frac{1}{2} (1 + 4\pi^2 f^2 \tau^2)^{\frac{1}{2}} \right]^{\frac{1}{2}}, \quad (1)$$

where  $g_0$  is the conductance and  $\tau$  is the life time of carriers, we successfully reproduce the current noise power spectrum density as shown in Fig. 4. For the calculation  $g_0$  was taken neglecting the leak current observed as the initial hump. The carrier life time was taken from a literature to be  $2.7 \times 10^{-5}\text{s}$ . From the good agreement of the calculated  $S_i$  with Eq. (1), we conclude that

measured non- $1/f$  noise is attributed to the shot noise. The frequency where noise starts to increase at about  $f = 10\text{kHz}$  is determined by the carrier life time  $\tau$ .  $S_i$  at 100Hz and 100kHz as a function of applied bias are compared in Fig. 5a. For all measured conditions, calculation results agree well with measurements. Fig. 5b shows the recombination current used for the calculation together with the simulated barrier height at the  $p-i-n$  junction with MEDICI. From Fig. 5b, it is seen that the recombination current diminishes rapidly as  $V_{pn}$  reaches to the built-in potentials and diminishes the potential barrier.

It is expected that shot noise would be no more observable if the potential barrier disappears. Fig. 6 shows exactly the case in the measurement. The shot noise increases according to the bias increase. However, beyond  $V_{pn}=0.8\text{V}$ , the noise reduces to the conventional feature without the shot noise.

### 3. Discussion and Conclusion

We have investigated shot noise arising from a  $p-i-n$  junction for the purpose of understanding the shot noise feature. It is very much dependent on the carrier transport mechanism to surmount the potential barrier, which can be characterized by the carrier life time.

Simulated potential distribution of a MOSFET with the pocket implantation is shown in Fig. 7a. Significant potential barriers are induced due to the high impurity concentration of the pocket. The barrier height reaches even 0.2V at 20nm down from the surface. At the source side enough carrier exists even at the 20nm depth as shown in Fig. 7b, and thus the shot noise is expected to be measured.

### Acknowledgment

The  $p-i-n$  diodes were fabricated at the Research Center for Nanodevices and Systems, Hiroshima University. The authors would like to acknowledge the members of the center for their help in device fabrication and fruitful discussions.

### References

- [1] M. S. Obrecht et al., *Jpn. J. Appl. Phys.* **39**, 1690 (2000); *IEEE Trans. Electron Devices* **49**, 524 (2002) and references therein.
- [2] MEDICI User's Manual, Synopsys Inc.
- [3] A. van der Ziel, *Noise in Solid State Devices and Circuits* (John Wiley & Sons, New York, 1981); Y. Yamamoto, *Fundamentals of Noise Processes* <http://feynman.stanford.edu/EEAP248.html>

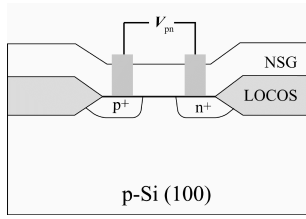


Figure 1: Structure of fabricated *p-i-n* diode.

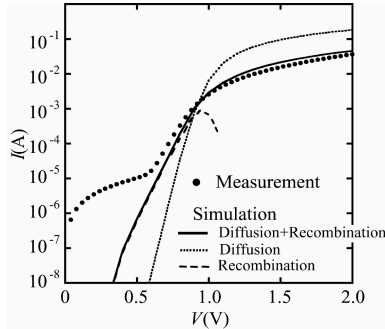


Figure 2: Measured *I-V* characteristics in comparison with MEDICI simulations. The current is composed of diffusion + drift and recombination components.

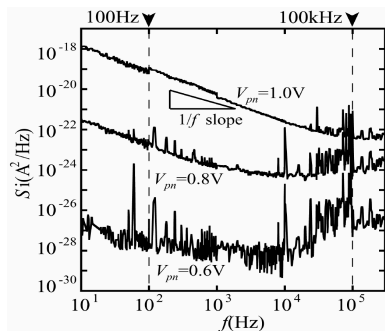


Figure 3: Measured noise power densities for different applied biases. Noise increases under higher frequency under lower applied bias.

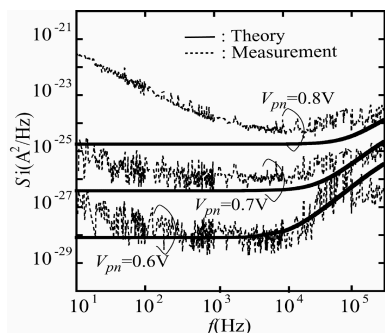


Figure 4: Calculated noise densities with shot noise included as a function of applied bias in comparison with measured values.

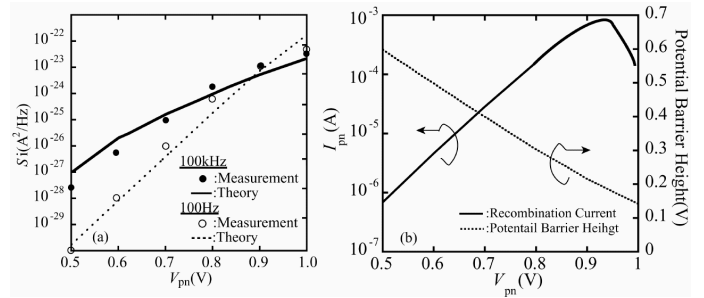


Figure 5: (a) Comparison of calculated noise power density as a function of applied bias for 100Hz and 100kHz. (b) Calculated recombination current and potential barrier height in the *p-i-n* device.

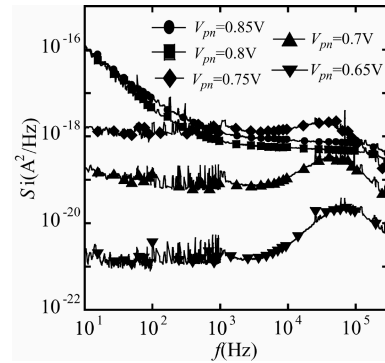


Figure 6: Noise power density as a function of frequency for different applied biases. Show noise increases according the bias increase. At biases greater than 0.8V, shot noise is no longer observable.

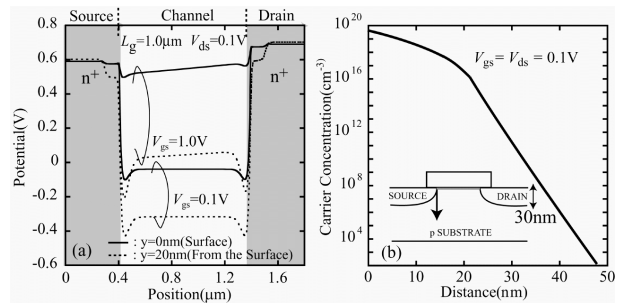


Figure 7: (a) Potential curves in a MOSFET for different applied biases. The potentials at the surface and at 20nm below the surface are plotted. (b) Carrier concentration at the source junction in the depth direction depicted by the arrow. Carriers are present down to 20nm in the substrate.